Theoretical prediction of structural, electronic and optical properties of quaternary alloy $Zn_{1-x}Be_xS_ySe_{1-y}$

Hacini K[a)], Meradji H[a)†], Ghemid S[a)], and El Haj Hassan F[b)]

[a)] *Laboratoire LPR, Département de Physique, Faculté des Sciences, Université de Annaba, Algeria*

[b)] *Laboratoire de physique des Matériaux, Faculté des Sciences, Université Libanaise, Elhadath, Beirut, Lebanon*

(Received 24 May 2011; revised manuscript received 7 October 2011)

Within density functional theory based on the full potential-linearized augmented plane wave method, we carry out the first-principles calculation of the structural, electronic, and optical properties of the zinc blende quaternary alloy $Zn_{1-x}Be_xS_ySe_{1-y}$. The Perdew–Burke–Ernzerhof generalized gradient approximation based on the optimization of total energy and the Engel–Vosko generalized gradient approximation based on the optimization of the corresponding potential are used. Our investigation on the effect of the composition on lattice constants, bulk modulus, band gap, optical dielectric constant, and refractive index shows a non-linear dependence. The energy gap $E_g(x, y)$ has been determined over the entire compositions x and y. In addition, the energy band gap of the technologically important quaternary alloy $Zn_{1-x}Be_xS_ySe_{1-y}$ in conditions of being lattice matched to ZnS substrate has been investigated. It is noteworthy that the present work is the first theoretical study of the quaternary alloy of interest.

Keywords: density functional theory, full potential-linearized augmented plane wave method, quaternary alloy, lattice-matched substrate

PACS: 61.66.Dk, 71.15.Ap, 71.15.Nc, 71.15.Mb **DOI:** 10.1088/1674-1056/21/3/036102

1. Introduction

The semiconductor alloys provide a natural means of tuning the magnitude of the forbidden gap and other material parameters so as to optimize semiconductor devices and widen their application. Quaternary systems open new possibilities for material engineering as they enable the control of three basic parameters: the band gap, the lattice constant, and the valence band offset. Consequently, the fabrication procedure is very important in optoelectronic engineering.

Recently, practical applications of the semiconductor alloys fabricated on the basis of II–VI compounds have become very widespread. To develop these alloys for use as optoelectronic devices, such as short-wavelength lasers and ultraviolet detectors, we need new and improved materials with a wider range of band gap as well as a higher stacking fault energy than that obtained from elemental or compound semiconductors.[1] Additionally, long standing problems such as the achievement of stable and low-resistivity p-type doping, high-longevity Ohmic contact, and low defect density for the ternary and quaternary alloys should be solved.[2]

Beryllium (Be) chalcogenide semiconductor alloys have recently been proposed for improving the performance of ZnSe-based blue-green lasers.[3] According to the theoretical calculation and subsequent experimental verification, the II–VI compounds containing Be have been found to possess an enhanced ability to significantly reduce the defect propagation due to stronger covalent bondings and lattice hardening.[3,4] The strong covalent bonding in Be-based II–VI compounds supports a considerable lattice hardening, which avoids the multiplication of defects during the operation of II–VI semiconductor laser devices.[5,6]

Recently, the technological importance of the group (Zn, Be) (S, Se) particularly for optoelectronic devices has stimulated the study of their quaternary alloy $Zn_{1-x}Be_xS_ySe_{1-y}$. This system has a special importance in that it will provide a higher band gap for detecting ultraviolet rays. To the best of our knowledge, there are no theoretical and experimental reports about the $Zn_{1-x}Be_xS_ySe_{1-y}$ alloy. Hence, to provide a basis for understanding the future device concepts and applications, we have com-

†Corresponding author. E-mail: hmeradji@yahoo.fr

© 2012 Chinese Physical Society and IOP Publishing Ltd

puted the structural, electronic, and optical properties of $Zn_{1-x}Be_xS_ySe_{1-y}$ quaternary alloy using the full potential-linearized augmented plane wave (FP-LAPW) method within density functional theory (DFT).

In the present work, we focus our attention on the variation of lattice constant, bulk modulus, band gap, and refractive index of composition (x, y). Then, the gap energy of $Zn_{1-x}Be_xS_ySe_{1-y}$ at the lattice constant of ZnS has been calculated. The organization of this paper is as follows: we present the computational method called FP-LAPW in Section 2. In Section 3, we report and discuss the calculated structural and electronic properties of the investigated quaternary alloys and their related binary compounds and ternary alloys. Finally, conclusions are given in Section 4.

2. Theoretical aspect and computational method

In this work, we have used the self consistent FP-LAPW method within the DFT to solve the Khon–Sham equations as implanted in the WIEN2K code.[7] In this program , space is divided into two regions, and spherical muffin-tins (MTs) surround the nuclei. The radial solutions of the Schrödinger equation and their energy derivatives are used as basis functions. There is an interstitial region between the MTs, where the basis set consists of plane waves. There is no pseudopotential approximation and core states are calculated self-consistently in the crystal potential. The core states are fully relativistic, while the valence and semicore states are treated semi-relativistically (i.e. ignoring spin-orbit coupling). In this method, an energy bound separating of -6 Ry between the valence electrons and the core states was chosen. The exchange correlation potential for the structural properties was calculated using the Perdew–Burke–Ernzerhof generalized gradient approximation (PBE-GGA),[8] while the Engel–Vosko generalized gradient approximation (EV-GGA)[9] was applied for the electronic properties.

In our calculations, we ensure that $R_{\mathrm{MT}} \cdot K_{\max} = 8$, which determines the matrix size (R_{MT} is the smallest of all atomic sphere radii, $K_{\max}$ is the cutoff of the interstitial plane wave). Values of R_{MT} were assumed to be 2.1, 1.8, 2, and 2.2 a.u. for Zn, Be, S, and Se atoms, respectively. A mesh of 55 special $\boldsymbol{k}$ points for binary compounds and 27 special $\boldsymbol{k}$ points for the alloys were taken in the irreducible wedge of the Brillouin zone for the energy calculation.

3. Results and discussion

3.1. Binary compounds

The quaternary compounds $Zn_{1-x}Be_xS_ySe_{1-y}$ are bordered by the ternary alloys $Zn_{1-x}Be_xS$, $Zn_{1-x}Be_xSe$, ZnS_xSe_{1-x}, and BeS_xSe_{1-x}, which are bounded, in turn, by four binary compounds of ZnS, ZnSe, BeS, and BeSe. A schematic diagram describing the calculation models is presented in Fig. 1. As the starting point, we have computed the structural and electronic properties of the binary compounds that crystallize in the two-atom unit cell zinc blende lattice structure. Fitting the Murnaghan equation of states[10] to the total energy versus many different volumes yields the equilibrium lattice parameters and bulk modulus. These results are tabulated in Table 1, along with the other experimental and theoretical values available. Considering the general trend that the GGA usually overestimates the lattice parameters,[22,23] our GGA results of binary compounds are in reasonable agreement with the experimental and other calculated values.

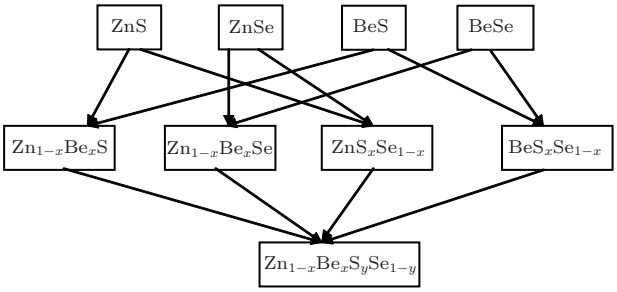


Fig. 1. Schematic diagram of the calculation models.

The computed band structures of the binary compounds using both GGA and EV-GGA schemes indicate a direct band gap $\Gamma \rightarrow \Gamma$ for ZnS and ZnSe and an indirect band gap $\Gamma \rightarrow X$ for BeS and BeSe. The results of the band gaps are given in Table 1. As expected, the band gap values given by the EV-GGA are in better agreement with available experimental results in comparison with the values calculated by GGA. In fact, it is well known that GGA underestimates the energy gap.[24,25] This is mainly due to the fact that the functionals within this approximation have simple forms that are not flexible enough to accurately reproduce both exchange-correlation energy and its charge derivative. It is noticeable that the Engel–Vosko scheme, which is based on potential optimization, is capable of giving a more reliable

band structure. However, for standard GGA, since the exchange-correlation energy is optimized, in general the structural properties can be reproduced more accurately.

Table 1. Calculated lattice parameter, bulk modulus, and band gap energy (E_g) for the binary compounds in the zinc blende structure at equilibrium volume.

	Lattice constant a/Å			Bulk modulus B/GPa			E_g/eV			
	Present work	Exp.	Other work	Present work	Exp.	Other work	Present work		Exp.	Other work
							GGA	EV		EV
ZnS	5.455	5.409[a)]	5.458[e)], 5.436[f)]	70.04	75.00[d)]	69.30[e)], 77.4[f)]	1.969	2.812	3.68[a)]	2.823[e)]
ZnSe	5.741	5.668[a)]	5.743[g)], 4.747[e)]	56.96	64.70[j)]	56.82[g)], 6.77[e)]	1.111	1.848	2.69[a)]	1.863[e)]
BeS	4.883	4.870[b)]	4.883[h)], 4.839[i)]	92.45	105.0[b)]	91.60[h)], 102.8[i)]	3.148	4.247	> 5.5[f)]	4.26[g)]
BeSe	5.184	5.137[c)]	5.178[h)], 5.137[i)]	75.19	92.20[c)]	79.66[h)], 82.2[i)]	2.672	3.634	4–4.5[f)]	3.64[g)]

[a)]Ref. [11], [b)]Ref. [12], [c)]Ref. [13], [d)]Ref. [14],[e)]Ref. [15],[f)]Ref. [16], [g)]Ref. [17],[h)]Ref. [18],[i)]Ref. [19],[j)]Ref. [20], [k)]Ref. [21].

3.2. Ternary alloys

The second step of our simulation was to study the ternary alloys: $Zn_{1-x}Be_xS$, $Zn_{1-x}Be_xSe$, ZnS_xSe_{1-x}, and BeS_xSe_{1-x}. We have used ordered structures described in terms of supercells with eight atoms per unit cell, for the compositions $x = 0.25$, 0.5, 0.75. For the considered structures, we performed the structural optimization by minimizing the total energy with respect to the cell parameters and the atomic positions.

Our calculated lattice constants of different compositions of ZnS_xSe_{1-x} and BeS_xSe_{1-x} alloys, as shown in Fig. 2, were found to vary almost linearly with concentration following the Vegard's law (i.e., a linear variation of the lattice constant of alloys versus composition x[26]) with marginal upward bowing parameters of −0.034 (−0.027 Å in Ref. [15]) and −0.036 Å, respectively. While, a large deviation from the Vegard's law was found for $Zn_{1-x}Be_xS$ and $Zn_{1-x}Be_xSe$ alloys with upward bowing parameters of −0.197 (−0.16651 Å in Ref. [17], −0.16 Å in Ref. [27]) and −0.213 Å (−0.1678 Å in Ref. [17], −0.1314 Å in Ref. [27]). However, deviations from Vegard's law in semiconductor alloys have been reported both experimentally[28] and theoretically.[18] The physical origin of this deviation should be mainly due to the large mismatch of the lattice constants of the relevant binary compounds.

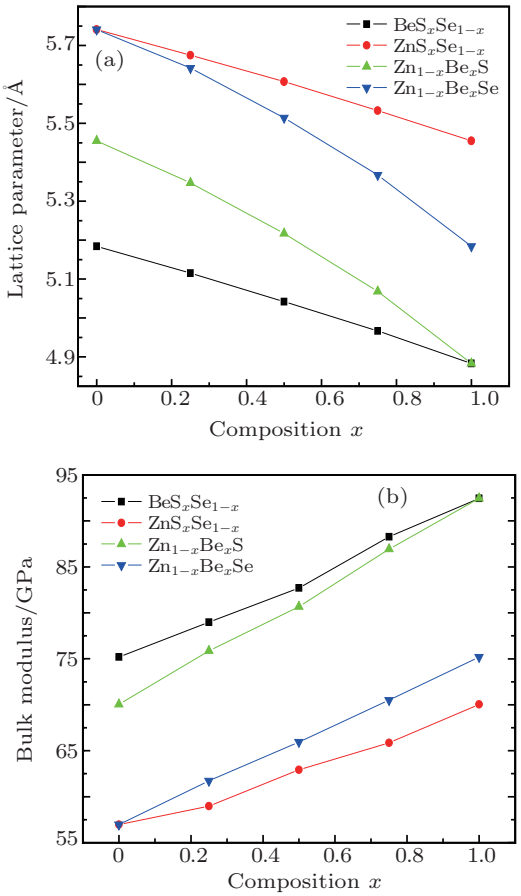


Fig. 2. (colour online) Composition dependence of the calculated lattice constant (a) and bulk modulus (b) for the four pseudo-binary alloys using PBE-GGA.

A deviation of the bulk modulus from the linear concentration dependence (LCD) (see Fig. 2) with downward bowings of 3.824 (Ref. [15]: 2.12 GPa), 3.017, 0.978 (Ref. [17]: 0.8573 GPa), and 0.238 GPa (Ref. [17]: 0.8573 GPa) for ZnS_xSe_{1-x}, BeS_xSe_{1-x}, $Zn_{1-x}Be_xS$, and $Zn_{1-x}Be_xSe$ alloys was observed. A

more precise comparison of the behaviours of these ternary alloys (see Fig. 2) shows that the decrease of the lattice constant is accompanied by the increase of the bulk modulus. It represents bond strengthening or weakening effects induced by changing the composition.

Figure 3 displays the variations of the direct and indirect band gap energies as functions of the composition x for the ternary alloys. Note that all band gap energies exhibit non-linear behaviour with respect to x with different rates of variation. Particular attention has been devoted to the crossover point, at which the Γ and X valley minima have the same energy. Thus, for $Zn_{1-x}Be_xS$ and $Zn_{1-x}Be_xSe$ alloys, the band gap undergoes a crossover from direct to indirect at a certain value of x. For this purpose, we have calculated the direct and indirect band gaps for the alloys at various concentrations. The direct-to-indirect (Γ–$\Gamma \rightarrow \Gamma$–$X$) band gap crossovers have been located by using the EV-GGA scheme at concentrations of 0.81 (Ref. [17]: 0.76) and 0.80 (Ref. [17]: 0.79), respectively.

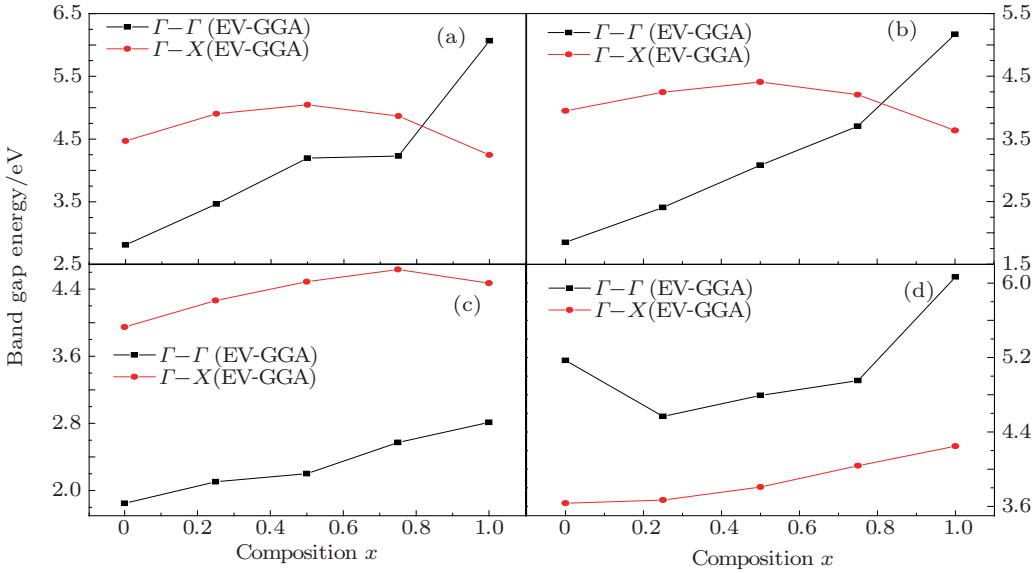


Fig. 3. (colour online) Energy band gap as functions of the composition x for the ternary alloys: (a) $Zn_{1-x}Be_xS$, (b) $Zn_{1-x}Be_xSe$, (c) ZnS_xSe_{1-x}, (d) BeS_xSe_{1-x}.

The band gap energies increase nonlinearly with increasing concentration x, providing a positive gap bowing. Indeed, it is a general trend for the band gap of an alloy $A_xB_{1-x}C$ in terms of the pure compound energy gaps E_{AC} and E_{BC} following the semi-empirical formula:

$$E_g = xE_{AC} + (1-x)E_{BC} - x(1-x)b_E, \qquad (1)$$

where the curvature b_E is commonly known as a gap bowing parameter. Based on the EV-GGA scheme, the calculated bowing parameters of ZnS_xSe_{1-x}, BeS_xSe_{1-x}, $Zn_{1-x}Be_xS$, and $Zn_{1-x}Be_xSe$ alloys are equal to 0.275 (Ref. [11]: 0.68), 3.845, 1.93, and 2.02 (Ref. [29]: 0.97) eV for E_g^{Γ} (at Γ point), respectively.

3.3. Quaternary $Zn_{1-x}Be_xS_ySe_{1-y}$ alloys

In order to compute the lattice parameter, bulk modulus, energy band gap, and refractive index of the quaternary alloys $Zn_{1-x}Be_xS_ySe_{1-y}$, we adopted the special quasi-random structures (SQS) approach. The supercells used in our calculations were thus obtained via a simulated-annealing procedure. Among 64 atom simple cubic structures, the ones that minimize the total energy with respect to the cell parameters and the atomic positions were searched. The results concerning the lattice constant and bulk modulus are depicted in Figs. 4 and 5, respectively. A marginal deviation of the lattice constant from the Vegard's law as well as that of the bulk modulus from the LCD can be observed.

The formation energy $E_{\rm Form}(x,y)$ of quaternary alloys at different concentrations was calculated using the following formula:

$$\begin{aligned} E_{\rm Form}(x,y) = {} & E_{\rm ZnBeSSe}(x,y) - xyE_{\rm BeS} \\ & + (1-x)yE_{\rm ZnS} + x(1-y)E_{\rm BeSe} \\ & + (1-x)(1-y)E_{\rm ZnSe}, \end{aligned} \quad (2)$$

where $E_{\rm BeS}$, $E_{\rm ZnS}$, $E_{\rm BeSe}$, and $E_{\rm ZnSe}$ are the total energies of the corresponding binary compounds, and $E_{\rm ZnBeSSe}$ is the total energy of the quaternary alloy at relevant concentrations. Figure 5 shows the results in a contour plot form, the darker part of the graph corresponds to more stable alloy. It is apparent that the least stable alloys are those with concentration near 50% for Be and 70% for S.

We have also investigated the electronic structures of these alloys. The alloy wave functions at the top of the valance and the bottom of the conduction bands have a Γ character. The largest direct band gap EV-GGA value calculated for the quaternary alloys is 3.9 eV at composition $x = y = 0.75$. In view of Fig. 4, one can note that the band gap energies depend nonlinearly on the compositions, especially at high concentration of x and y.

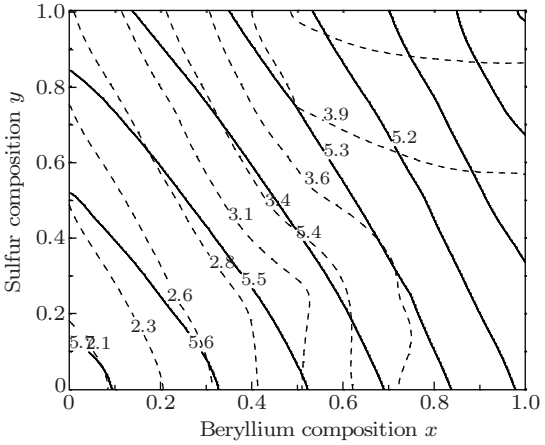


Fig. 4. Contour map of the calculated lattice constant in Å (solid lines) and direct-indirect minimum energy band gap in eV (dashed lines) versus the compositions x and y for $Zn_{1-x}Be_xS_ySe_{1-y}$ quaternary alloys.

Table 2. Calculated lattice parameter, bulk modulus, and band gap energy ($E_{\rm g}$) for the $Zn_{1-x}Be_xS_ySe_{1-y}$ quaternary alloys.

x	y	Lattice constant a/Å	Bulk modulus B/GPa	$E_{\rm g}$/eV	
				GGA	EV
0.25	0.25	5.573	65.48	1.819	2.630
0.25	0.5	5.502	67.59	2.036	2.872
0.25	0.75	5.427	71.55	2.292	3.155
0.5	0.25	5.454	69.47	2.463	3.003
0.5	0.5	5.373	72.52	2.891	3.552
0.5	0.75	5.297	76.24	2.971	3.890
0.75	0.25	5.299	73.89	2.731	3.676
0.75	0.5	5.224	77.73	2.824	3.789
0.75	0.75	5.148	82.74	2.994	3.991

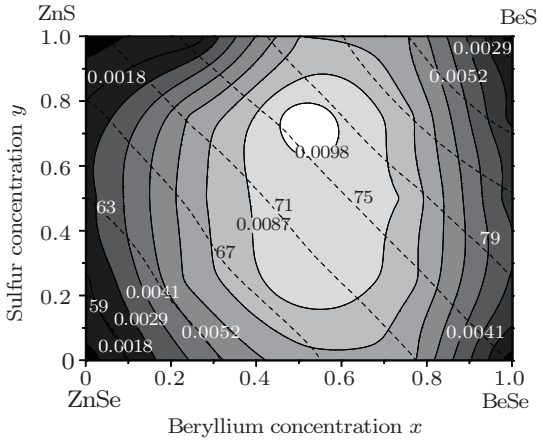


Fig. 5. Contour map of the calculated bulk modulus in GPa (dashed lines) and formation energy contour lines (Ry per cell) (solid lines and shadings) versus the compositions x and y for $Zn_{1-x}Be_xS_ySe_{1-y}$ quaternary alloys.

Figure 4 can be very useful for engineering of semiconductor alloys because it enables us to select alloys with desirable optical properties on any given substrate by looking for concentration at which the system has the required lattice constant and band gap.

The optical properties of a solid are usually described in terms of the complex dielectric function $\varepsilon(\omega) = \varepsilon_1(\omega) + \mathrm{i}\,\varepsilon_2(\omega)$. The imaginary part of the dielectric function in the long wavelength limit can be obtained directly from the electronic structure calculation, using the joint density of states and the optical matrix elements. The real part of the dielectric function can be derived from the imaginary part using the Kramers–Kronig relationship. The acquirement of both real and imaginary parts of the dielectric function allows the calculation of important optical func-

tions. The refractive index is given by

$$n(\omega) = \left[\frac{\varepsilon_1(\omega)}{2} + \frac{\sqrt{\varepsilon_1^2(\omega) + \varepsilon_2^2(\omega)}}{2}\right]^{1/2}. \quad (3)$$

At low frequency ($\omega = 0$), we obtain the following relation:

$$n(0) = \varepsilon^{1/2}(0). \quad (4)$$

The refractive index of semiconductors represents a fundamental physical aspect that characterizes their optical and electronic properties. The knowledge of the refractive index is essential for devices such as photonic crystals, wave guides, solar cells and detectors.[30]

Figure 6 displays the contour map of the calculated refractive index versus the compositions x and y for $Zn_{1-x}Be_xS_ySe_{1-y}$ quaternary alloys. One can note that the refractive index decreases with increasing x and y, and depends nonlinearly on the compositions.

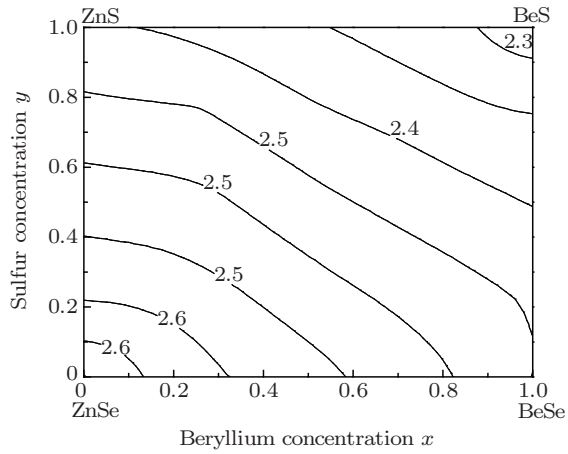


Fig. 6. Contour map of the calculated refractive index versus the compositions x and y for $Zn_{1-x}Be_xS_ySe_{1-y}$ quaternary alloys.

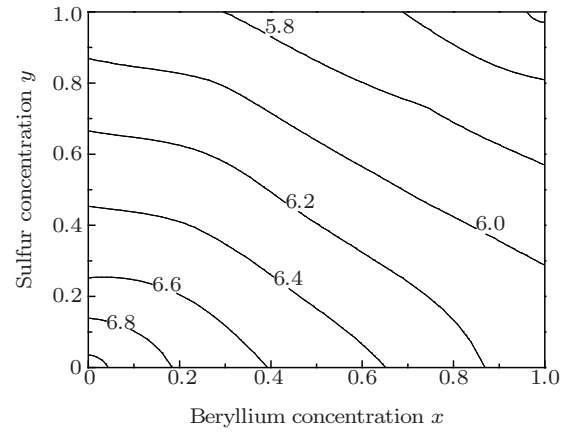


Fig. 7. Contour map of the calculated dielectric function versus the compositions x and y for $Zn_{1-x}Be_xS_ySe_{1-y}$ quaternary alloys.

The dielectric function has been estimated according to Eq. (4). The results are given in Fig. 7. Qualitatively, the composition dependence of the dielectric function of the alloy has the same trend as that of the refractive index. This is not surprising because the dielectric function is directly calculated by using Eq. (4).

Finally, in order to understand the interfaces of our investigated alloys and the proximity effects of substrates on them, we present the properties of $Zn_{1-x}Be_xS_ySe_{1-y}$ alloys with lattice matched to ZnS semiconductor substrate. For this purpose, we used the following relationship between the compositions x and y for lattice matched to quaternary alloys:

$$\begin{aligned} a(x,y) = {} & xya_{\mathrm{BeS}} + (1-x)ya_{\mathrm{ZnS}} + x(1-y)a_{\mathrm{BeSe}} \\ & + (1-x)(1-y)a_{\mathrm{ZnSe}}, \end{aligned} \quad (5)$$

where a_{BeS}, a_{BeSe}, a_{ZnSe}, and a_{ZnS} are the lattice constants of the binary compounds. By equalizing $a(x,y)$ and the lattice constant of ZnS, the corresponding concentration for lattice matched to quaternary alloy $Zn_{1-x}Be_xS_ySe_{1-y}$ is obtained as follows:

$$y = \frac{0.286 - 0.557x}{0.286 + 0.015x}, \quad (0 \le x \le 0.5). \quad (6)$$

The above expression, specifies a (x, y) relationship in which the corresponding alloy have the same lattice constant value as for ZnS. We considered five different concentrations along the line of lattice matched to ZnS: (x, y)=(0/32, 32/32), (7/32, 19/32), (10/32,13/32), (13/32,7/32), (16/32, 1/32).

Figure 8 displays the energy gaps as functions of BeS compositions along the ZnS matching lines of the

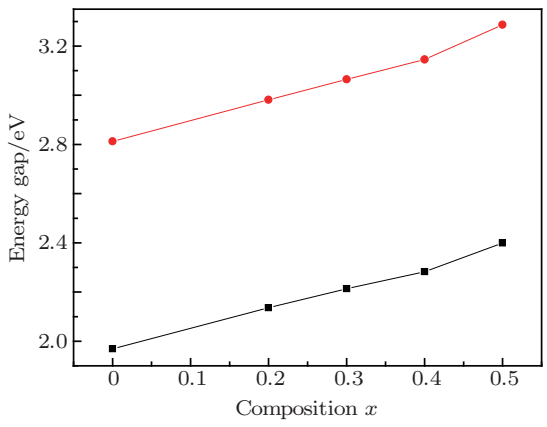


Fig. 8. (colour online) Energy band gaps of $Zn_{1-x}Be_xS_ySe_{1-y}$ quaternary alloy lattice matched to ZnS as functions of composition x using EV-GGA (solid circles) and GGA (solid squares) schemes.

composition plane, which is obtained from a calculation performed by GGA and EV-GGA schemes. The visible nonlinear behaviour of the band gap versus concentration x leads to the gap bowing parameter of 0.494 eV within the EV-GGA.

The results show that by tuning the concentrations in quaternary alloys, a broad range of band gaps (covering the ultraviolet window) and therefore optical properties are accessible for alloys grown on ZnS substrate. Within the EV-GGA, the calculated band gap of $Zn_{1-x}Be_xS_ySe_{1-y}$ lattice matched to ZnS varies from 2.812 to 3.286 eV. From our results, we find that the studied quaternary alloys can be useful in the design of new blue–green laser diodes and laser-emitting diodes.

4. Conclusion

In summary, we have investigated the structural, electronic, and optical properties of $Zn_{1-x}Be_xS_ySe_{1-y}$ quaternary alloys as functions of the compositions x and y using the FP-LAPW method within the DFT. A nonlinear behaviour of the lattice constants, bulk modulus, band gap, dielectric function, and refractive index with respect to x and y has been observed. The calculations of formation energy shows that the least stable alloys are around 50% and 70% concentrations of Be and S atoms, respectively. The gap bowing of quaternary alloys is strong at high composition x. The direct band gap of the ZnBeSSe lattice matched to ZnS for the range of the composition x from 0 to 0.5 has been calculated, the results indicate that the band gap increases with the composition x.

References

[1] Long D and Schmit J L 1970 *Semiconductors and Semimetals* (New York: Academic Press) p.175

[2] Chauvet C, Bousquet V, Tournié E and Faurie J P 1999 *J. Electron. Mater.* **28** 662

[3] Waag A, Fischer F, Schull K, Barron T, Lugauer H J, Litz T, Zehneder U, Ossau W, Gerhard T, Keim M, Reuscher G and Landwehr G 1997 *Appl. Phys. Lett.* **70** 280

[4] Zhang J Y, Shem D Z, Fan X W, Yang B J and Zheng Z H 2000 *J. Cryst. Growth* **214-215** 100

[5] Munoz A, Rodriguez-Hernandez P and Mujica A 1996 *Phys. Stat. Sol.* **198** 439

[6] Waag A, Fischer F, Lugauer H J, Litz T, Laubender J, Lunz U, Zehneder U, Ossau W, Gerhard T, Moller M and Landwehr G 1996 *J. Appl. Phys.* **80** 792

[7] Blaha P, Schwarz K, Madsen G K H, Kvasnicka D and Luitz J 2001 *WIEN2K* An Augmented Plane Wave + Local Orbitals Program for Calculating Crystal Properties, Karlheinz Schwarz (Techn. Universität, Austria, Vienna)

[8] Perdew J P, Burke S and Ernzerhof M 1997 *Phys. Rev. Lett.* **78** 1396(E)

[9] Engel E and Vosko S H 1993 *Phys. Rev.* B **47** 13164

[10] Murnaghan F D 1944 *Proc. Natl. Acad. Sci.* **30** 5390

[11] Okuyama H, Kishita Y and Ishibashi A 1998 *Phys. Rev.* B **57** 2257

[12] Narayana C, Nesamong V J and Ruoff A L 1997 *Phys. Rev.* B **56** 14338

[13] Luo H, Ghandehair K, Greene R G, Ruoff A L, Trail S S and Disalvo F J 1995 *Phys. Rev.* B **52** 7058

[14] Ves S, Schwartz U, Christensen N E, Syassen K and Cardona M 1990 *Phys. Rev.* B **42** 9113

[15] El Haj Hassan F, Amrani B and Bahsoun F 2007 *Physica* B **391** 365

[16] Lee S G and Chang K J 995 *Phys. Rev.* B **52** 1918

[17] Baaziz H, Charifi Z, El Haj Hassan F, Hashemifar S J and Akbarzadeh H 2006 *Phys. Stat. Sol.* (b) **243** 1296

[18] El Haj Hassan F 2005 *Phys. Stat. Sol.* (b) **242** 911

[19] Kalpana G, Pari G, Mookerjee A and Bhattacharyya A K 1998 *Int. J. Mod. Phys.* B **12** 1975

[20] Lee B H 1970 *J. Appl. Phys.* **44** 2984

[21] Yim W M, Dismukes J P, Stofko E J and Poff R J 1972 *J. Phys. Chem. Solids* **33** 501

[22] El Haj Hassan F, Amrani B and Bahsoun F 2007 *J. Phys.: Condensed Matter* **19** 386234

[23] El Haj Hassan F and Akbarzadeh H 2006 *Comput. Mater. Sci.* **35** 423

[24] Okoye C M I 2004 *Eu. Phys. J.* B **39** 5

[25] Ozaki S and Adachi S 1994 *J. Appl. Phys.* **75** 7470

[26] Vegard L 1921 *Z. Phys.* **5** 17

[27] Ameri M, Rached D, Rabah M, El Haj Hassan F, Khenata R and Doui-Aici M 2007 *Phys. Stat. Sol.* (b) **245** 106

[28] Jobst J, Hommel D, Lunz U, Gerhard T and Landwehr G 1996 *Appl. Phys. Lett.* **69** 97

[29] Chauvet C, Tournié E and Faurie J P 2000 *Phys. Rev.* B **61** 5332

[30] Ravindra N M, Ganapathy P and Choi J 2007 *Infrared. Phys. Technol.* **50** 21